

Emergent ferromagnetism in ZnO/Al₂O₃ core-shell nanowires : towards oxide spinterfaces

Xing, G. Z.; Wang, D. D.; Cheng, C.-J.; He, M.; Li, S.; Wu, T.

2013

Xing, G. Z., Wang, D. D., Cheng, C.-J., He, M., Li, S., & Wu, T. (2013). Emergent ferromagnetism in ZnO/Al₂O₃ core-shell nanowires : towards oxide spinterfaces. *Applied physics letters*, 103(2), 022402-.

<https://hdl.handle.net/10356/100094>

<https://doi.org/10.1063/1.4813217>

© 2013 AIP Publishing LLC. This paper was published in *Applied Physics Letters* and is made available as an electronic reprint (preprint) with permission of AIP Publishing LLC. The paper can be found at the following official DOI: [<http://dx.doi.org/10.1063/1.4813217>]. One print or electronic copy may be made for personal use only. Systematic or multiple reproduction, distribution to multiple locations via electronic or other means, duplication of any material in this paper for a fee or for commercial purposes, or modification of the content of the paper is prohibited and is subject to penalties under law.

Downloaded on 25 Aug 2022 01:36:32 SGT



Emergent ferromagnetism in ZnO/Al₂O₃ core-shell nanowires: Towards oxide spinterfaces

G. Z. Xing, D. D. Wang, C.-J. Cheng, M. He, S. Li, and T. Wu

Citation: [Applied Physics Letters](#) **103**, 022402 (2013); doi: 10.1063/1.4813217

View online: <http://dx.doi.org/10.1063/1.4813217>

View Table of Contents: <http://scitation.aip.org/content/aip/journal/apl/103/2?ver=pdfcov>

Published by the [AIP Publishing](#)



Re-register for Table of Content Alerts

Create a profile.



Sign up today!



Emergent ferromagnetism in ZnO/Al₂O₃ core-shell nanowires: Towards oxide spinterfaces

G. Z. Xing,^{1,2} D. D. Wang,¹ C.-J. Cheng,¹ M. He,¹ S. Li,² and T. Wu^{3,a)}

¹*Division of Physics and Applied Physics, School of Physical and Mathematical Sciences, Nanyang Technological University, Singapore 637371, Singapore*

²*School of Materials Science and Engineering, The University of New South Wales, Sydney, New South Wales 2052, Australia*

³*Division of Physical Sciences and Engineering, King Abdullah University of Science and Technology, Thuwal 23955-6900, Saudi Arabia*

(Received 22 May 2013; accepted 20 June 2013; published online 8 July 2013)

We report that room-temperature ferromagnetism emerges at the interface formed between ZnO nanowire core and Al₂O₃ shell although both constituents show mainly diamagnetism. The interface-based ferromagnetism can be further enhanced by annealing the ZnO/Al₂O₃ core-shell nanowires and activating the formation of ZnAl₂O₄ phase as a result of interfacial solid-state reaction. High-temperature measurements indicate that the magnetic order is thermally stable up to 750 K. Transmission electron microscopy studies reveal the annealing-induced jagged interfaces, and the extensive structural defects appear to be relevant to the emergent magnetism. Our study suggests that tailoring the spinterfaces in nanostructure-harnessed wide-band-gap oxides is an effective route towards engineered nanoscale architecture with enhanced magnetic properties.

© 2013 AIP Publishing LLC. [<http://dx.doi.org/10.1063/1.4813217>]

Bringing the spin degree of freedom into semiconductor devices has attracted much attention as a promising route towards semiconductor-based spintronics.^{1,2} As a prototypical oxide semiconductor, ZnO is an important wide-band-gap material with a large exciton binding energy (~ 60 meV), promising many applications in areas like optoelectronics and transparent electronics.^{3,4} Recently, there have been reports that ferromagnetism can be stabilized in transition (or rare-earth)-metal-doped ZnO,^{5–12} in spite of the fact that defect-free ZnO is nonmagnetic.¹³ However, the ferromagnetism in such doped oxides is generally rather weak, and the results are often controversial. It is clear that the conventional mechanisms such as the super- or double-exchange interactions cannot serve as the dominant scenario because the doping level is generally too low to produce a long-range magnetic order. On the other hand, there emerges a consensus that the magnetism in wide-band-gap oxides is often closely linked to the existence of structural impurities like point defects, grain boundaries, interfaces, and so on.^{14–20} In terms of mechanism, alternation of the electronic configuration, which is often a consequence of either intentional or unintentional structural/chemical inhomogeneity introduced in sample synthesis, has been proven as a viable approach to induce ferromagnetism.^{21–23} In particular, Coey *et al.* proposed that shallow donor electrons can form spin-split impurity bands and bound magnetic polarons.²⁴ However, the main challenge remains regarding how to harness the oxide nanostructures to produce an enhanced and reliable magnetism in order to become relevant to practical spintronic devices.²⁵

One viable approach of tailoring the magnetic order is to introduce interfaces between two different compounds in nanostructured oxide semiconductors. This approach is a drastic departure from the single-phase materials mostly reported

in literature and offers additional advantages. In fact, constructing interfaces between two oxide materials, e.g., LaAlO₃/SrTiO₃,²⁶ SrTiO₃/KTaO₃,²⁷ and La_{2/3}Ca_{1/3}MnO₃/MnO₃/YBa₂Cu₃O₇,²⁸ have led to a surge of research interest in the study of magnetic and electronic properties of oxide interfaces. Recently, engineering the ZnO surface has played important roles in modulating the spin polarization and magnetic order in several material systems including ZnO nanostructures with organic molecule-passivation.^{21–23,25,29} In fact, Zn K-edge X-ray magnetic circular dichroism measurements revealed a ferromagnetic-like contribution from the interface formed between the ZnO nanoparticle core and the organic molecules.²³ Similarly, spontaneous magnetization and hysteresis were observed in ZnO nanowires (NWs) modified with thiol-capped Ag nanoclusters³⁰ and in ZnO/ZnS core-shell nanoparticles.³¹ Moreover, such a kind of “spinterfaces” was discovered at the interface of strained ZnO films grown on quartz substrates,³² where the structural strain was suggested to play an important role. It is also worth mentioning that, as a route to molecular spintronics, spinterfaces with a high degree of spin polarization were also investigated in the context of organic/metallic layers.^{33–35}

In this Letter, we present an effective route towards the goal of enhanced magnetism by preparing and tailoring ZnO/Al₂O₃ (AZO) core-shell NWs, which have not only high surface-to-volume ratios but also large interface areas. The as-grown ZnO NWs showed a negligible magnetism as a result of high crystalline quality, whereas a clear ferromagnetic signal was detected after coating with a homogeneous Al₂O₃ outer shell, which can be further enhanced via annealing treatments. Our results suggest that nanoscale interface engineering and structural modification are effective to alter the local electronic and magnetic orders in core-shell NWs of wide-band-gap oxides and offer an alternative approach to produce magnetic nanostructures.

^{a)}Electronic mail: tao.wu@kaust.edu.sa

Single-crystal ZnO NWs were prepared in a horizontal tube furnace by means of vapor transport, and the experimental setup was described in previous reports.^{36–38} A homogeneous Al₂O₃ shell with various thicknesses was coated by using atomic layer deposition (ALD). In detail, the Si substrates covered with as-synthesized ZnO NWs were transferred to the ALD chamber [Beneq system (TFS 200)] and prebaked at 200 °C for 60 min in vacuum (1.5×10^{-1} Torr) with a steady Ar stream. The deposition took place at 200 °C using trimethylaluminum [Al(CH₃)₃] and water as the aluminum and the oxygen sources, respectively. The thickness of the Al₂O₃ shell was controlled by the number of precursor/purge cycles. Some samples of ZnO/Al₂O₃ core-shell NWs were then annealed in air at 800 °C for 3 h to activate the interfacial solid-state reaction. Magnetization measurements were performed on NW samples by using a superconducting quantum interference devices magnetometer (SQUID, Quantum Design, MPMSXL-5). Only plastic tweezers were used throughout all experiments to avoid any unintentional metal contamination. To determine the weight of NWs, the NWs were etched off after the SQUID experiments, and the substrate weight was accurately measured and deducted from the whole sample weight.

As shown in the field emission scanning electron microscopy (FESEM) image in Fig. 1(a), the as-grown ZnO NWs (sample uncoated ZnO (UZO)) on Si substrate have diameters of 50–100 nm and lengths of $\sim 2 \mu\text{m}$. The NWs became clearly thicker after a ~ 15 nm Al₂O₃ layer was coated (sample AZO) [Fig. 1(b)]. We further annealed the core-shell NWs in air at 800 °C for 3 h. Interestingly, we found that the annealed ZnO/Al₂O₃ core-shell NWs (sample A-AZO) show very rough surfaces [Fig. 1(c)]. In the X-ray diffraction (XRD) patterns of the as-grown and the coated ZnO NWs [Fig. 1(d)], all peaks can be identified with the crystalline wurtzite ZnO structure, while the Al₂O₃ shell is amorphous. However, after annealing, ZnAl₂O₄ phase with the spinel structure notably emerged although its intensity is weak [Fig. 1(e)]. ZnAl₂O₄ is a well-known wide-band-gap

semiconductor with an optical band gap of 3.8 eV, with applications such as photoelectronic devices.³⁹ Thus, we can conclude that notable solid state reaction occurs in the interface areas by the annealing treatments.

Figure 2(a) depicts the *M-H* curves measured on UZO, AZO, and A-AZO at 5 and 300 K. The annealed sample A-AZO exhibits a much higher magnetism than the as-coated sample AZO, whereas the magnetism in the as-grown uncoated NW sample UZO is the weakest. In the data, the diamagnetic signal from Si substrates without NWs was carefully measured and then subtracted from the raw data [Fig. 2(b)]. The saturation magnetism of the sample A-AZO reaches 0.046 emu/g. Because the sample contains multiple compositions, we cannot accurately determine the magnetism in terms of formula unit. Nevertheless, the observed value of saturation magnetization in A-AZO is comparable to what reported for nanograined ZnO films (0.05 emu/g),¹² but much higher than those of undoped ZnO nanoparticles obtained via chemical routes (between 0.0015 and 0.0022 emu/g)^{40,41} and ZnO nanorods (0.004 emu/g),⁴² as well as the thiol-capped ZnO nanoparticles (0.003 emu/g).²⁰

To find out the origin of magnetism in the annealed ZnO/Al₂O₃ core-shell NWs, we measured a control sample of ZnAl₂O₄ nanocrystals, which were fabricated using the conventional solid state reaction route from high-purity ZnO and Al₂O₃ powders, and found that ZnAl₂O₄ nanocrystals exhibits only a diamagnetic behavior [Fig. 2(c)]. Therefore, the enhanced magnetism in A-AZO cannot be attributed to the ZnAl₂O₄ nanocrystals alone formed at the ZnO/Al₂O₃ interface during annealing. Furthermore, we measured a few ZnO/Al₂O₃ NW samples with different thicknesses of Al₂O₃ shell, but did not find any considerable difference [Fig. 2(d)]. It further allows us to conclude that the observed ferromagnetism originates from ZnO/Al₂O₃ interfaces instead of the coated Al₂O₃ layers.

We measured the temperature dependent magnetization (*M-T*) curves of the ZnO/Al₂O₃ core-shell NW samples under a magnetic field of 500 Oe under both zero-field-cooled (ZFC) and field-cooled (FC) conditions. As shown in the inset of Fig. 2(e), in accordance with the *M-H* data, the temperature-dependent magnetization of A-AZO is much stronger than that of AZO. Furthermore, we carried out the high-temperature *M-T* experiments in an oven attached to the SQUID magnetometer, and as shown in Fig. 2(f), the magnetization of the sample A-AZO shows a transition close to 750 K, suggesting the magnetic order of the sample persists over a quite wide temperature range.

To understand the annealing-induced structural transformation at the interfaces within the ZnO/Al₂O₃ NWs, we carried out detailed transmission electron microscopy (TEM) experiments. As shown in Fig. 3(a), the as-grown ZnO NWs exhibit a single-crystal wurtzite structure and a [001] growth direction. After coating the amorphous alumina layer, the ZnO/Al₂O₃ core-shell structure was clearly observed, and there is no void or gap formed at the interface [Fig. 3(b)]. The local composition of the core-shell NWs was further confirmed in the energy-dispersive X-ray spectra with line scans of intensity profiles. Most importantly, after annealing treatment in air at 800 °C for 3 h, significant solid state reactions occurred at the interface regions, and the surfaces of

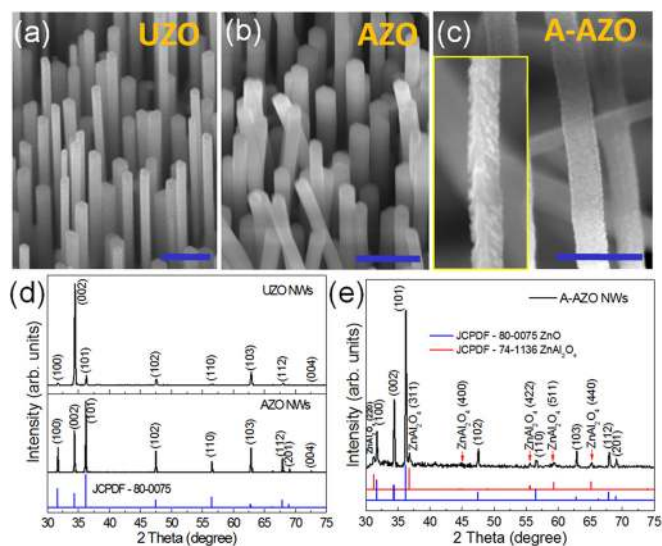


FIG. 1. FESEM images of (a) uncoated ZnO NWs (UZO), (b) ZnO/Al₂O₃ (AZO), and (c) annealed (A-AZO) core-shell structured NWs. The scale bars are 300 nm. (d) and (e) Corresponding XRD patterns.

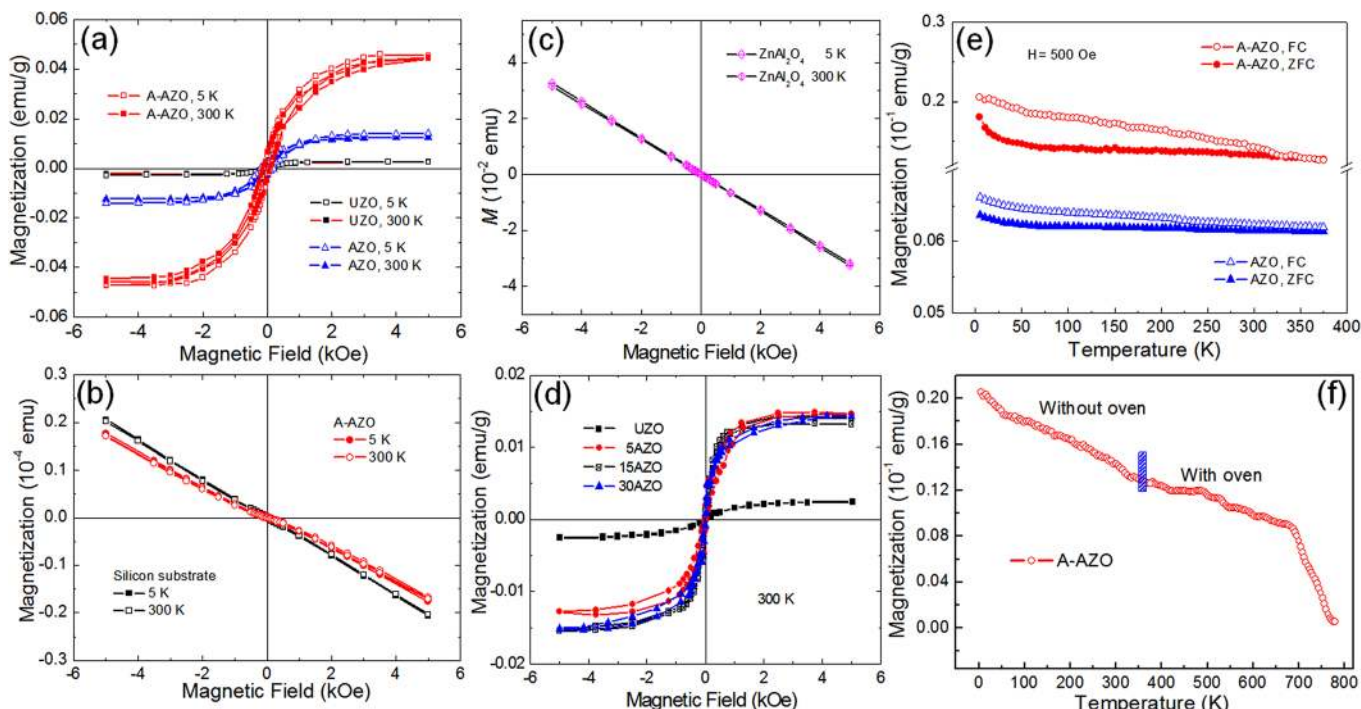


FIG. 2. (a) M - H loops of UZO, AZO, and A-AZO NWs measured at 5 and 300 K. (b) Raw M - H data measured on the annealed core-shell nanowire sample A-AZO without subtracting the diamagnetic substrate contribution. The diamagnetic signal of a bare Si substrate is also shown. (c) M - H loops of a control sample of ZnAl_2O_4 nanocrystals. (d) RT M - H data of as-grown NWs (UZO) and three $\text{ZnO}/\text{Al}_2\text{O}_3$ core-shell samples (AZO) with various Al_2O_3 thickness: 5, 15, and 30 nm. (e) ZFC and FC temperature-dependent magnetization curves of A-AZO and AZO measured in the temperature range of 5–380 K. (f) M - T curve of the A-AZO sample in the extended temperature range of 5–780 K.

the ZnO NWs become much rougher [Fig. 3(c)]. In the inset of Fig. 3(c), the ZnAl_2O_4 phase was clearly observed, which presumably resulted from nanoscale solid-state reaction between ZnO and Al_2O_3 within the NWs. The extensive high-resolution TEM (HRTEM) studies revealed the existence of lots of stacking faults and disordered structures in

the interface areas [Fig. 3(d)]. It is important to note that nanoscale ZnAl_2O_4 phase have a good lattice match with the ZnO core, as suggested by the selective-area electron diffraction (SAED) pattern shown in the inset of Fig. 3(c), and the atomic stacking at the epitaxial interface is illustrated in Fig. 4(a). Our SAED results also suggest that the Al_2O_3 shell remains amorphous in all samples.

Our comparative structure-property studies on three kinds of NW samples revealed an intriguing interface-related origin of the ferromagnetism in wide-band-gap oxides without any intentional doping of transition metals. Ferromagnetism has been observed previously in undoped thin films and nanoparticles of TiO_2 , HfO_2 , In_2O_3 , CaO , and CeO_2 .^{43,44} This phenomenon is generally recognized as the d^0 magnetism,^{45–49} and its origin is usually linked to structural defects.^{43,44,50} But the d^0 magnetism is usually very weak, comparable to the magnetic signal observed in our as-grown ZnO NW sample (UZO). The SQUID data in Fig. 2 reveal a clear trend: The ferromagnetism can be enhanced by coating the ZnO NWs with a thin amorphous alumina layer (shown for the sample AZO), which can be further strengthened by the annealing treatment (shown for the sample A-AZO). It is in line with the findings by Garcia *et al.*, where capping ZnO nanoparticles with different organic molecules was found to induce room-temperature ferromagnetic-like behaviors.^{21–23} In general, surfaces naturally break down the periodic boundary conditions which are assumed for ideal solids with infinite dimensions; thus, they are structural imperfection by themselves. Therefore, many structural motifs related to surfaces or grain boundaries can sustain a macroscopic magnetic order, particularly in nanomaterials.^{14,51–54}

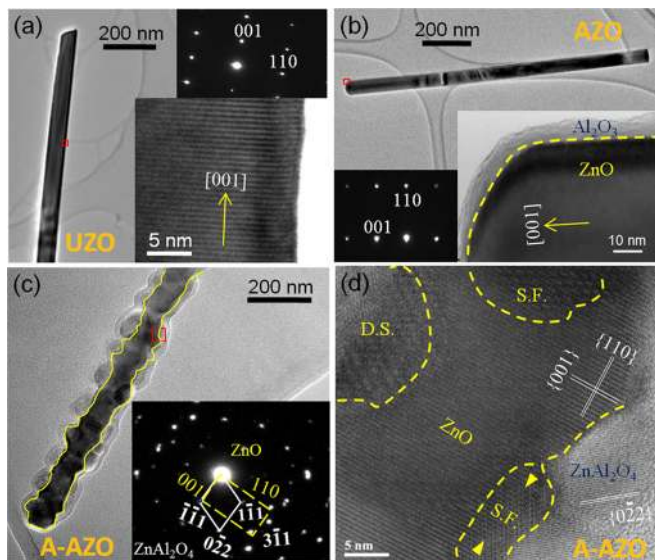


FIG. 3. TEM images of individual NWs of (a) the as-grown sample (UZO), (b) after Al_2O_3 coating (AZO), and (c) the annealed $\text{Al}_2\text{O}_3/\text{ZnO}$ core-shell nanowire sample (A-AZO). Insets show the corresponding SAED patterns and HRTEM images. The dashed line in the HRTEM image in (b) marks the $\text{Al}_2\text{O}_3/\text{ZnO}$ interface. The thin solid line highlights the boundary of the rough ZnO nanowire core after reacting with the Al_2O_3 shell. (d) Close-up HRTEM image of an A-AZO NW, showing regions of stacking faults (S.F.) and disordered structures (D.S.) as well as the ZnAl_2O_4 phase at the interface area.

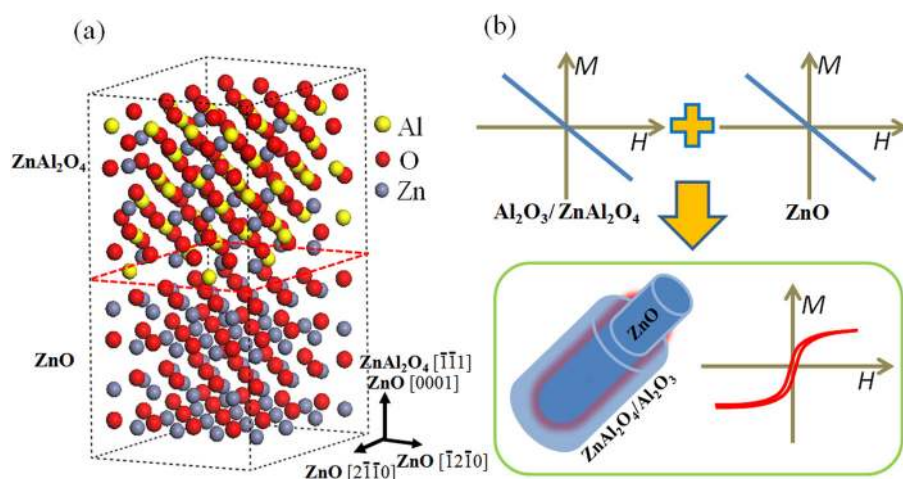


FIG. 4. (a) Schematic illustration of the epitaxial interface between ZnO and ZnAl₂O₄ with their atomic crystal structures. (b) Illustration of the concept of producing magnetism in core-shell structured NWs of ZnO core wrapped by ZnAl₂O₄/Al₂O₃ shell. It is noted that the individual components exhibit mainly diamagnetism, but ferromagnetism emerges in nanostructures with engineered “spinterfaces.”

In our annealed core-shell NWs, there are not only large-area surfaces but also extended jagged interfaces, which presumably contribute to the overall ferromagnetism. In the interface regions, unpaired electrons from the extended defect complexes may play important roles in establishing the local magnetic order,¹² and the magnetic hysteresis is dominated by magnetic dipole interactions instead of the conventional magnetocrystalline anisotropy.⁵⁵ It is not surprising that the electronic structure is severely altered on the nanoscale at the interfaces between the nanocrystalline ZnO, Al₂O₃, and ZnAl₂O₄ grains. Consequently, the unbalanced spin-dependent density of states at the Fermi surface gives rise to the observed magnetic moments. Furthermore, in ionic oxides like ZnO, the localized nature of the oxygen 2*p* states can lead to strong spin-exchange interactions, which may be further enhanced in nanomaterials.⁴¹

Our design strategy towards magnetic nanostructures is illustrated in Fig. 4(b). It is important to note that local strain and structural imperfections are always abundantly present in the multi-phase nanostructures like the annealed core-shell NWs discussed here, and the complexity of electronic and magnetic orders is expected to result in interesting physical properties. On the other hand, it is clear that only a small portion of the synthesized materials, particularly near the interface areas, presents ferromagnetism, whereas the rest remains diamagnetic. In a recent x-ray spectroscopic study, we showed that most of transition metal ions in doped ZnO are antiferromagnetically coupled, contributing no macroscopic magnetism.⁵⁶ In general, the magnetism and anisotropy in doped transition-metal oxides as a result of magnetic bound polarons are weak.^{57–59} Furthermore, in Co-doped ZnO nanocrystals⁶⁰ and Co-doped TiO₂ thin films,⁶¹ paramagnetism and superparamagnetism were observed and attributed to the formation of metallic nanoclusters. Nevertheless, the experimental revelation of the interface magnetism or “spinterface” in multi-component nanomaterials presented here clearly warrants further theoretical and spectroscopic investigations.

In summary, we presented our experimental results that the magnetic properties of undoped ZnO NWs can be significantly tailored and enhanced by forming core-shell nanostructures and conducting post-synthesis annealing treatments. The extended structural defects as well as the nanoscale formation of new ternary phases in the interface areas give rise to the alternation of local chemical and

electronic configurations in such engineered oxide nanostructures. We hope that the demonstrated strategy of producing emergent magnetic order at the interfaces between nonmagnetic components of wide-band-gap oxides may stimulate the search for other oxide nanoscale architectures and devices with interesting properties.

This work was supported in part by the National Research Foundation, Singapore, through Grant NRF-CRP4-2008-04, as well as by the Vice-Chancellor’s Research Program (SIR50/PS26746), Faculty of Science Research Grant (IR001/PS30560) and ARC FT100100956 at University of New South Wales. D. D. Wang acknowledges the research support fund of 2011M500861. We also thank M. N. Liu and H. J. Fan for performing the ALD coatings.

¹S. A. Wolf, D. D. Awschalom, R. A. Buhrman, J. M. Daughton, S. von Molnar, M. L. Roukes, A. Y. Chtchelkanova, and D. M. Treger, *Science* **294**, 1488 (2001).

²I. Žutić, J. Fabian, and S. Das Sarma, *Rev. Mod. Phys.* **76**, 323 (2004).

³Ü. Özgür, Y. I. Alivov, C. Liu, A. Teke, M. A. Reshchikov, S. Dogan, V. Avrutin, S. J. Cho, and H. Morko, *J. Appl. Phys.* **98**, 041301 (2005).

⁴C. Klingshirn, *ChemPhysChem* **8**, 782 (2007).

⁵K. Ando, H. Saito, Z. Jin, T. Fukumura, M. Kawasaki, Y. Matsumoto, and H. Koinuma, *J. Appl. Phys.* **89**, 7284 (2001).

⁶A. Walsh, J. L. F. Da Silva, and S. H. Wei, *Phys. Rev. Lett.* **100**, 256401 (2008).

⁷G. Z. Xing, J. B. Yi, J. G. Tao, T. Liu, L. M. Wong, Z. Zhang, G. P. Li, S. J. Wang, J. Ding, T. C. Sum, C. H. A. Huan, and T. Wu, *Adv. Mater.* **20**, 3521 (2008).

⁸T. Dietl, H. Ohno, F. Matsukura, J. Cibert, and D. Ferrand, *Science* **287**, 1019 (2000).

⁹M. Venkatesan, C. B. Fitzgerald, J. G. Lunney, and J. M. D. Coey, *Phys. Rev. Lett.* **93**, 177206 (2004).

¹⁰X. F. Wang, F. Q. Song, Q. Chen, T. Y. Wang, J. L. Wang, P. Liu, M. R. Shen, J. G. Wan, G. H. Wang, and J. B. Xu, *J. Am. Chem. Soc.* **132**, 6492 (2010).

¹¹Y. F. Tian, Y. F. Li, M. He, I. A. Putra, H. Y. Peng, B. Yao, S. A. Cheong, and T. Wu, *Appl. Phys. Lett.* **98**, 162503 (2011).

¹²D. D. Wang, Q. Chen, G. Z. Xing, J. B. Yi, S. B. Rahman, J. Ding, J. L. Wang, and T. Wu, *Nano Lett.* **12**, 3994 (2012).

¹³M. Venkatesan, C. B. Fitzgerald, and J. M. D. Coey, *Nature* **430**, 630 (2004).

¹⁴A. Sundaresan, R. Bhargavi, N. Rangarajan, U. Siddesh, and C. N. R. Rao, *Phys. Rev. B* **74**, 161306 (2006).

¹⁵Y. W. Ma, J. Ding, D. C. Qi, J. B. Yi, H. M. Fan, H. Gong, A. T. S. Wee, and A. Rusydi, *Appl. Phys. Lett.* **95**, 072501 (2009).

¹⁶S. B. Ogale, *Adv. Mater.* **22**, 3125 (2010).

¹⁷J. B. Yi, H. Pan, J. Y. Lin, J. Ding, Y. P. Feng, S. Thongmee, T. Liu, H. Gong, and L. Wang, *Adv. Mater.* **20**, 1170 (2008).

- ¹⁸R. Podila, W. Queen, A. Nath, J. T. Arantes, A. L. Schoenhalz, A. Fazzio, G. M. Dalpian, J. He, S. J. Hwu, M. J. Skove, and A. M. Rao, *Nano Lett.* **10**, 1383 (2010).
- ¹⁹Y. F. Li, R. Deng, Y. F. Tian, B. Yao, and T. Wu, *Appl. Phys. Lett.* **100**, 172402 (2012).
- ²⁰B. Y. Zhang, Y. F. Li, A. M. Liu, Z. Z. Zhang, B. H. Li, G. Z. Xing, T. Wu, X. B. Qin, D. X. Zhao, C. X. Shan, and D. Z. Shen, *Appl. Phys. Lett.* **99**, 182503 (2011).
- ²¹M. A. García, J. M. Merino, E. F. Pinel, A. Quesada, J. d. I. Venta, M. L. R. Gonzalez, G. R. Castro, P. Crespo, J. Llopis, J. M. Gonzalez-Calbet, and A. Hernando, *Nano Lett.* **7**, 1489 (2007).
- ²²J. Chaboy, R. Boada, C. Piquer, M. A. Laguna-Marco, M. García-Hernández, N. Carmona, J. Llopis, M. L. Ruiz-González, J. González-Calbet, J. F. Fernández, and M. A. García, *Phys. Rev. B* **82**, 064411 (2010).
- ²³C. Guglieri, M. A. Laguna-Marco, M. A. García, N. Carmona, E. Céspedes, M. García-Hernández, A. Espinosa, and J. Chaboy, *J. Phys. Chem. C* **116**, 6608 (2012).
- ²⁴J. M. D. Coey, M. Venkatesan, and C. B. Fitzgerald, *Nat. Mater.* **4**, 173 (2005).
- ²⁵Y. F. Tian, S. R. Bakaul, and T. Wu, *Nanoscale* **4**, 1529 (2012).
- ²⁶A. Ohtomo and H. Y. Hwang, *Nature* **427**, 423 (2004).
- ²⁷R. Oja, M. Tyunina, L. Yao, T. Pinomaa, T. Kocourek, A. Dejneka, O. Stupakov, M. Jelinek, V. Trepakov, S. van Dijken, and R. M. Nieminen, *Phys. Rev. Lett.* **109**, 127207 (2012).
- ²⁸J. Chakhalian, J. W. Freeland, G. Srajer, J. Stremper, G. Khaliullin, J. C. Cezar, T. Charlton, R. Dalgliesh, C. Bernhard, G. Cristiani, H.-U. Habermeier, and B. Keimer *Nat. Phys.* **2**, 244 (2006).
- ²⁹S. Z. Deng, H. M. Fan, M. Wang, M. R. Zheng, J. B. Yi, R. Q. Wu, H. R. Tan, C. H. Sow, J. Ding, Y. P. Feng, and K. P. Loh, *ACS Nano* **4**, 495 (2010).
- ³⁰S. Deng, K. P. Loh, J. B. Yi, J. Ding, H. R. Tan, M. Lin, Y. L. Foo, M. Zheng, and C. H. Sow, *Appl. Phys. Lett.* **93**, 193111 (2008).
- ³¹Y. Yazaki, M. Suda, N. Kameyama, and Y. Einaga, *Chem. Lett.* **39**, 594 (2010).
- ³²C. S. Ong, T. S. Herng, X. L. Huang, Y. P. Feng, and J. Ding, *J. Phys. Chem. C* **116**, 610 (2012).
- ³³F. Djeghloul, F. Ibrahim, M. Cantoni, M. Bowen, L. Joly, S. Boukari, P. Ohresser, F. Bertran, P. Le Fèvre, P. Thakur, F. Scheurer, T. Miyamachi, R. Mattana, P. Seneor, A. Jaafar, C. Rinaldi, S. Javaid, J. Arabski, J.-P. Kappler, W. Wulfhekel, N. B. Brookes, R. Bertacco, A. Taleb-Ibrahimi, M. Alouani, E. Beaupaire, and W. Weber, *Sci. Rep.* **3**, 1272 (2013).
- ³⁴S. Sanvito, *Nat. Phys.* **6**, 562 (2010).
- ³⁵K. V. Raman, A. M. Kamerbeek, A. Mukherjee, N. Atodiresi, T. K. Sen, P. Lazić, V. Caciuc, R. Michel, D. Stalke, S. K. Mandal, S. Blügel, M. Müntzenberg, and J. S. Moodera, *Nature* **493**, 509 (2013).
- ³⁶G. Z. Xing, X. S. Fang, Z. Zhang, D. D. Wang, X. Huang, J. Guo, L. Liao, Z. Zheng, H. R. Xu, T. Yu, Z. X. Shen, C. H. A. Huan, T. C. Sum, H. Zhang, and T. Wu, *Nanotechnology* **21**, 255701 (2010).
- ³⁷G. Z. Xing, D. D. Wang, J. B. Yi, L. L. Yang, M. Gao, M. He, J. H. Yang, J. Ding, T. C. Sum, and T. Wu, *Appl. Phys. Lett.* **96**, 112511 (2010).
- ³⁸G. Z. Xing, J. B. Yi, D. D. Wang, L. Liao, T. Yu, Z. X. Shen, C. H. A. Huan, T. C. Sum, J. Ding, and T. Wu, *Phys. Rev. B* **79**, 174406 (2009).
- ³⁹T. El-Nabarawy, A. A. Attia, and M. N. Alaya, *Mater. Lett.* **24**, 319 (1995).
- ⁴⁰D. Sanyal, M. Chakrabarti, T. K. Roy, and A. Chakrabarti, *Phys. Lett. A* **371**, 482 (2007).
- ⁴¹X. Y. Xu, C. X. Xu, J. Dai, J. G. Hu, F. J. Li, and S. Zhang, *J. Phys. Chem. C* **116**, 8813 (2012).
- ⁴²Z. J. Yan, Y. W. Ma, D. L. Wang, J. H. Wang, Z. S. Gao, L. Wang, P. Yu, and T. Song, *Appl. Phys. Lett.* **92**, 081911 (2008).
- ⁴³G. Z. Xing, Y. H. Lu, Y. F. Tian, J. B. Yi, C. C. Lim, Y. F. Li, G. P. Li, D. D. Wang, B. Yao, J. Ding, Y. P. Yuan, and T. Wu, *AIP Adv.* **1**, 022152 (2011).
- ⁴⁴N. H. Hong, J. Sakai, N. Poirot, and V. Brizé, *Phys. Rev. B* **73**, 132404 (2006).
- ⁴⁵J. M. D. Coey, *Solid State Sci.* **7**, 660 (2005).
- ⁴⁶K. S. Yang, R. Q. Wu, L. Shen, Y. P. Feng, Y. Dai, and B. B. Huang, *Phys. Rev. B* **81**, 125211 (2010).
- ⁴⁷W. A. Adeagbo, G. Fischer, A. Ernst, and W. Hergert, *J. Phys.: Condens. Matter* **22**, 436002 (2010).
- ⁴⁸A. Droghetti, C. D. Pemmaraju, and S. Sanvito, *Phys. Rev. B* **78**, 140404(R) (2008).
- ⁴⁹S. Banerjee, M. Mandal, N. Gayathri, and M. Sardar, *Appl. Phys. Lett.* **91**, 182501 (2007).
- ⁵⁰A. Sundaresan and C. N. R. Rao, *Nanotoday* **4**, 96 (2009).
- ⁵¹L. Y. Li, Y. H. Cheng, X. G. Luo, H. Liu, G. H. Wen, R. K. Zheng, and S. P. Ringer, *Nanotechnology* **21**, 145705 (2010).
- ⁵²Z. Zhang, J. B. Yi, J. Ding, L. M. Wong, H. L. Seng, S. J. Wang, J. G. Tao, G. P. Li, G. Z. Xing, T. C. Sum, C. H. A. Huan, and T. Wu, *J. Phys. Chem. C* **112**, 9579 (2008).
- ⁵³C. Guglieri and J. Chaboy, *J. Phys. Chem. C* **114**, 19629 (2010).
- ⁵⁴H. W. Peng, H. J. Xiang, S. H. Wei, S. S. Li, J. B. Xia, and J. B. Li, *Phys. Rev. Lett.* **102**, 17201 (2009).
- ⁵⁵J. M. D. Coey, J. Mlack, M. Venkatesan, and P. Stamenov, *IEEE Trans. Mag.* **46**, 2501 (2010).
- ⁵⁶T. Kataoka, Y. Yamazaki, V. R. Singh, A. Fujimori, F.-H. Chang, H.-J. Lin, D. J. Huang, C. T. Chen, G. Z. Xing, J. W. Seo, C. Panagopoulos, and T. Wu, *Phys. Rev. B* **84**, 153203 (2011).
- ⁵⁷M. He, Y. Tian, D. Springer, I. Putra, G. Z. Xing, E. Chia, S. A. Cheng, and T. Wu, *Appl. Phys. Lett.* **99**, 222511 (2011).
- ⁵⁸Y. F. Tian, Y. F. Li, and T. Wu, *Appl. Phys. Lett.* **99**, 222503 (2011).
- ⁵⁹Y. F. Li, R. Deng, G. Z. Xing, B. Yao and T. Wu, *Appl. Phys. Lett.* **97**, 102506 (2010).
- ⁶⁰Z. H. Wang, D. Y. Geng, S. Guo, W. J. Hu, and Z. D. Zhang, *Appl. Phys. Lett.* **92**, 242505 (2008).
- ⁶¹S. R. Shinde, S. B. Ogale, J. S. Higgins, H. Zheng, A. J. Millis, V. N. Kulkarni, R. Ramesh, R. L. Greene, and T. Venkatesan, *Phys. Rev. Lett.* **92**, 166601 (2004).